Model Predictive Control for the Operation of Building Cooling Systems

Yudong Ma, Francesco Borrelli, Brandon Hencey, Brian Coffey, Sorin Bengea, and Philip Haves

***Abstract*—This brief presents a model-based predictive control (MPC) approach to building cooling systems with thermal energy storage. We focus on buildings equipped with a water tank used for actively storing cold water produced by a series of chillers. First, simplified models of chillers, cooling towers, thermal storage tanks, and buildings are developed and validated for the purpose of model-based control design. Then an MPC for the chilling system operation is proposed to optimally store the thermal energy in the tank by using predictive knowledge of building loads and weather conditions. This brief addresses real-time implementation and feasibility issues of the MPC scheme by using a simplified hybrid model of the system, a periodic robust invariant set as terminal constraints, and a moving window blocking strategy. The controller is experimentally validated at the University of California, Merced. The experiments show a reduction in the central plant electricity cost and an improvement of its efficiency.**

***Index Terms*—Building energy, building modeling, model predictive control (MPC).**

I. Introduction

THE building sector consumes about 40% of the energy used in the United States and is responsible for nearly 40% of greenhouse gas emissions. It is therefore economically, socially and environmentally significant to reduce the energy consumption of buildings. For a wide range of innovative heating and cooling systems, their enhanced efficiency depends on the active storage of thermal energy.

This brief focuses on the modeling, control design and real time implementation of the thermal energy storage on the campus of the University of California, Merced. The campus cooling system consists of a chiller plant (three chillers redundantly configured as two in series, one backup in parallel), an array of cooling towers, a 7000 m^3 thermal energy storage tank, a primary distribution system and secondary distribution loops serving each building of the campus. The two series chillers are operated each night to recharge the storage tank which meets campus cooling demand the following day. Although the storage tank enables load shifting to off-peak hours to reduce peak demand, the lack of an optimized operation results in conservatively overcharging the tank, where heat losses erode efficiency, and in suboptimal operation of chillers and cooling towers.

The objective of this brief is to design a predictive controller in order to minimize energy consumption while satisfying the cooling demand of the campus and operational constraints. The main idea of model predictive control (MPC) is to use the model of the plant and buildings to predict the future evolution of the system [12], [16]. For complex constrained multi-variable control problems, model predictive control has become the accepted standard in the process industry [3]: its success is largely due to its almost unique ability to handle, simply and effectively, hard constraints on control and states.

The application of predictive optimal controllers for active and passive building thermal storage has been extensively studied in the past (see [6], [7], [9]–[11], [13], and references therein). In particular, Henze *et al.* [9] investigated predictive control design for a three-story office building equipped with two chillers with constant coefficient of performance and a thermal energy storage system. Oldewurtel *et al.* [18] investigated the integration of MPC and weather predictions to increase the energy efficiency in building climate control.

Compared to the aforementioned literature, the novel contributions of this work are: 1) the development of a simple switching nonlinear model for the storage tank which is identified and validated by historical data; 2) the systematic integration of weather prediction in the MPC design to optimize the chillers operation; and 3) the design of a low-complexity MPC scheme which is guaranteed to be robust against uncertain buildings load demands. In particular, a periodic moving window blocking strategy [4] is used to reduce the computational time associated with the resulting nonlinear constrained optimization. Also, robust persistent feasibility requires that the tank has always enough energy to satisfy a time-varying uncertain buildings cooling demand. Robust persistent feasibility is obtained in our scheme by using a time-varying periodic robust invariant set as terminal constraint [2].

This brief is organized as follows. Section II introduces the system and its simplified hybrid model. In Section III, the MPC control algorithm is outlined together with the move blocking strategy and the terminal set computation. Section IV details the experimental setups and procedures for controlling the plant. Experimental data are presented in Section V. Finally, conclusions are drawn in Section VI.

II. System Model

Fig. 1 shows the main components of the UC Merced Campus used to generate, store and distribute thermal energy. The system consists of a condenser loop, a primary loop, a secondary (campus) loop, and several tertiary (building) loops. The chilled water is generated via chillers and cooling towers within the primary and condenser loops. The chilled water is

Manuscript received October 01, 2010; accepted January 10, 2011. Manuscript received in final form March 01, 2011. Recommended by Associate Editor J. H. Lee. This work was supported in part by the Department of Energy, Lawrence Berkeley National Laboratories, and the NSF CAREER Award 0844456.

Y. Ma and F. Borrelli are with the Department of Mechanical Engineering, University of California, Berkeley, CA 94720-1740 USA (e-mail: myd07@berkeley.edu; fborrelli@berkeley.edu).

B. Hencey is with Sibley School of Mechanical and Aerospace Engineering, Cornell University Ithaca, NY 14853 USA.

B. Coffey is with the Department of Architecture, University of California, Berkeley, CA 94720-1800 USA.

S. Bengea is with United Technologies Research Center (UTRC), East Hartford, CT 06108 USA.

P. Haves is with Lawrence Berkeley National Lab, Berkeley, CA 94720 USA.

Digital Object Identifier 10.1109/TCST.2011.2124461

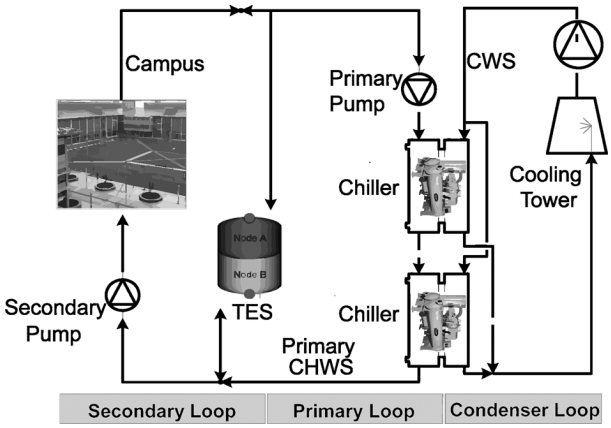

Fig. 1. Scheme plot of the chilling system.

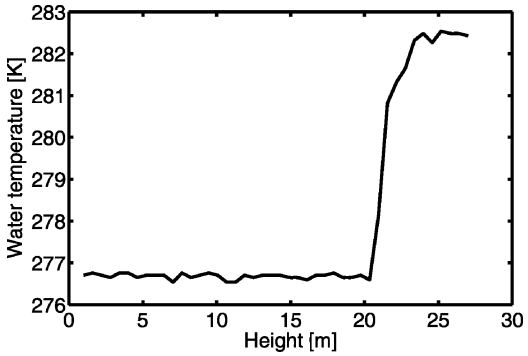

Fig. 2. Temperature distribution of water in the tank.

stored in a stratified thermal energy storage tank, and distributed to the buildings throughout the campus via the secondary loop. Internal building loops use pumps and valves to distribute the chilled water to the fan coils and air handling units (AHUs) that deliver cold air to the thermal zones. The chilled water is warmed by the air-side load of the buildings and returned to the secondary loop.

The following subsections present a dynamic model of the system. Our objective is to develop a simplified yet descriptive model which can be used for real time optimization in an MPC scheme.

A. Simplifying Assumptions

A1) The water in the tank is subject to minor mixing and thus can be modeled as a stratified system with layers of warmer water ($\sim$ 282.6 K) at the top and cooler water ($\sim$ 276.6 K) at the bottom. Fig. 2 depicts the temperature of the water measured by 44 sensors evenly installed inside the tank along the height of the tank at 8:30 am on the 29th of November, 2008. One can observe a thin layer of water, known as a thermocline that has a steep temperature gradient over the height of the tank. The thermocline is approximately 1.6 m high, has an average temperature of 279.5 K, and a gradient of 3.7 K/m. We lump warmer (cooler) water with temperature higher (lower) than 279.5 K above (below) the thermocline and denote the height and average temperature of this water as z_a and T_a (z_b and T_b), respectively. A four states system describing the heights and temperatures of the warmer and cooler water in the tank is obtained.

A2) Lower-level controllers actuate chillers and cooling towers in order to achieve a: 1) desired temperature of condenser water produced by cooling towers $T_{\mathrm{CWS,ref}}$; 2) mass flow rate of chilled water supplied by chillers $\dot{m}_{\mathrm{CHWS,ref}}$; and 3) chilled water temperature $T_{\mathrm{CHWS,ref}}$. We neglect the dynamics of controlled chillers and cooling towers, and assume that there is no tracking error between controlled variables and references: $T_{\mathrm{CWS}} = T_{\mathrm{CWS,ref}}$, $\dot{m}_{\mathrm{CHWS}} = \dot{m}_{\mathrm{CHWS,ref}}$, $T_{\mathrm{CHWS}} = T_{\mathrm{CHWS,ref}}$.

A3) The campus load is considered as a lumped disturbance in terms of heat flux required to cool down all buildings over the campus.

B. Main Subsystems of the Cooling System

Next we detail the system components and their models.

1) Chillers and Cooling Towers Model: Based on assumption A2, the power (P) used by the pumps, chillers, and the cooling towers is modeled as a static function of $T_{\mathrm{CHWS}}, T_{\mathrm{CWS}}$, $\dot{m}_{\mathrm{CHWS}}$ (described in assumption A2)

$$P = \mathrm{Power}(T_{\mathrm{CHWS}}, T_{\mathrm{CWS}}, \dot{m}_{\mathrm{CHWS}}, T_{wb}, T_{\mathrm{CHWR}}) \quad (1)$$

where T_{CHWR} is the chilled water return temperature, i.e., the temperature of the water that leaves the buildings, and that is stored at the top of the tank. T_{wb} is the temperature read from a wet bulb thermometer. The wet bulb temperature physically reflects the temperature and humidity of the ambient air.

The function $\mathrm{Power}(\cdot)$ is implemented as a 5-D lookup table obtained by extensive simulations of a high fidelity model of the chillers and cooling towers under various initial conditions.

2) Thermal Energy Storage Tank: According to assumption A1, the tank is part of a closed hydraulic loop, that is, the mass flow rate entering (exiting) the tank is equal to the mass flow rate exiting (entering) the tank. Subsequently, the height of water in the tank $z_a + z_b$ is a constant that equals to the height of the tank z_{tank}, where z_a is the height of warmer water and z_b is the height of cooler water. z_a and z_b are estimated according to A1.

The tank can operate in two modes depending on the control inputs (the chilled water flow rate $\dot{m}_{\mathrm{CHWS}}$) and the disturbances (the flow rate demanded by the campus $\dot{m}_{\mathrm{cmp},s}$).

Charging ($\dot{m}_{\mathrm{CHWS}} \geq \dot{m}_{\mathrm{cmp},s}$): If the flow rate $\dot{m}_{\mathrm{CHWS}}$ produced by the chiller is greater than the flow rate of chilled water supplied to the campus $\dot{m}_{\mathrm{cmp,s}}$, the difference will be charging the tank. By simple mass and energy conservation law, the tank dynamics in charging mode can be modeled as

$$\dot{H}_b = (\dot{m}_{\mathrm{CHWS}} - \dot{m}_{\mathrm{cmp},s}) C_p T_{\mathrm{CHWS}} \quad (2a)$$

$$\dot{H}_a = (\dot{m}_{\mathrm{cmp},s} - \dot{m}_{\mathrm{CHWS}}) C_p T_a \quad (2b)$$

$$T_{\mathrm{cmp},s} = T_{\mathrm{CHWS}} \quad (2c)$$

$$T_{\mathrm{CHWR}} = \frac{T_{\mathrm{cmp},r}\dot{m}_{\mathrm{cmp},s} - T_a(\dot{m}_{\mathrm{cmp},s} - \dot{m}_{\mathrm{CHWS}})}{\dot{m}_{\mathrm{CHWS}}} \quad (2d)$$

where $\dot{H}_a$ ($\dot{H}_b$) is enthalpy flow rate of the warmer (cooler) water, C_p is the specific heat of water, and $T_{\mathrm{cmp},s}$ ($T_{\mathrm{cmp},r}$) is

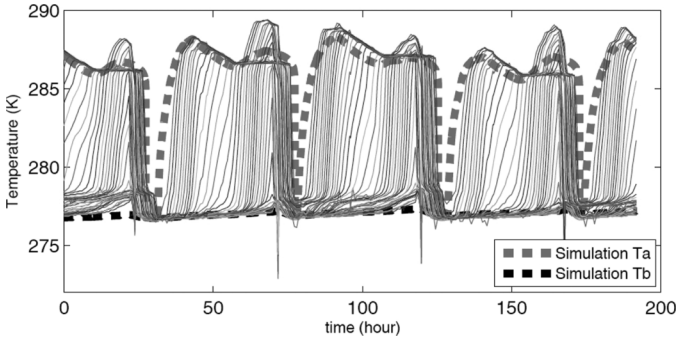

Fig. 3. Tank water temperature validation.

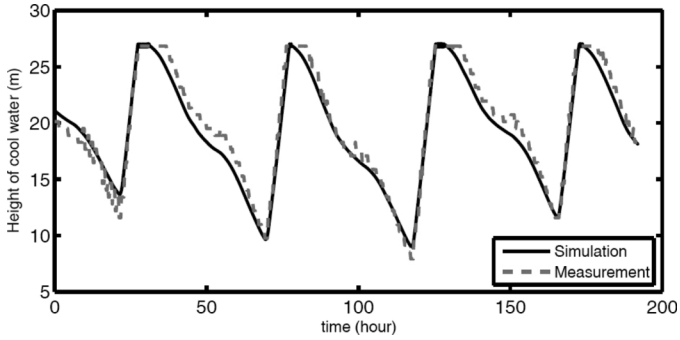

Fig. 4. Tank water height validation.

the temperature of water supplied to (returned from) campus, T_{CHWR} is the temperature of water entering the chillers.

Discharging ($\dot{m}_{\mathrm{CHWS}} \leq \dot{m}_{\mathrm{cmp},s}$): The tank will be discharged if the flow rate produced by the chiller $\dot{m}_{\mathrm{CHWS}}$ is less than campus flow rate $\dot{m}_{\mathrm{cmp},s}$. The following equations model the tank dynamics in discharging mode:

$$\dot{H}_a = (\dot{m}_{\mathrm{cmp},s} - \dot{m}_{\mathrm{CHWS}}) C_p T_{\mathrm{cmp},r} \tag{3a}$$

$$\dot{H}_b = (\dot{m}_{\mathrm{CHWS}} - \dot{m}_{\mathrm{cmp},s}) C_p T_b \tag{3b}$$

$$T_{\mathrm{CHWR}} = T_{\mathrm{cmp},r} \tag{3c}$$

$$T_{\mathrm{cmp},s} = \frac{T_{\mathrm{CHWS}} \dot{m}_{\mathrm{CHWS}} - T_b(\dot{m}_{\mathrm{CHWS}} - \dot{m}_{\mathrm{cmp},s})}{\dot{m}_{\mathrm{cmp},s}}. \tag{3d}$$

The mass and internal energy conservation laws hold in both modes

$$\dot{z}_b = \frac{\frac{(\dot{m}_{\mathrm{CHWS}} - \dot{m}_{\mathrm{cmp},s})}{\rho}}{\pi r_{\mathrm{tank}}^2},\ \dot{z}_a + \dot{z}_b = 0 \tag{4a}$$

$$\dot{U}_a = \dot{H}_a + \dot{Q}_{b>a} + \dot{Q}_{\mathrm{Amb}>a},\ \dot{U}_b = \dot{H}_b + \dot{Q}_{a>b} + \dot{Q}_{\mathrm{Amb}>b} \tag{4b}$$

where ρ is the water density, r_{tank} is the radius of the tank, $U_a = m_a C_p T_a$ (U_b) is the internal energy of warmer (cooler) water in the tank, $\dot{Q}_{\mathrm{Amb}>a}$ ($\dot{Q}_{\mathrm{Amb}>b}$) is the heat transferred from ambient to the warmer (cooler) water in the tank: $\dot{Q}_{\mathrm{Amb}>a} = (T_{\mathrm{amb}} - T_a)(2\pi r_{\mathrm{tank}} z_a)k_1$, $\dot{Q}_{a>b} = (T_a - T_b)(\pi r_{\mathrm{tank}}^2)k_2$ ($\dot{Q}_{b>a}$) is the heat conducted from warmer (cooler) water to cooler (warmer) water in the tank, and k_1, k_2 are the thermal conductivity coefficients.

The proposed model (2)–(4) is validated by using data collected in May 22–29, 2007. We applied the historical inputs to the tank model, and the output of the model $[z_a, z_b, T_a, T_b]$ is compared with the measurements (see Figs. 3 and 4).

Fig. 3 shows the tank water temperature validation results. The thin solid lines indicate the measurements of the 44 temperature sensors installed evenly along the height of the tank water, and the thick black dotted lines show the temperature of the cool (warm) water. The proposed tank model successfully matches the temperature dynamics of the top (bottom) layer of the tank water. However, the second peak of the top water temperature during the day is not captured due to the formation of a second thermocline (notice in Fig. 3 the bumps above 287 K everyday in the afternoon). A higher order model could overcome this limitation. We preferred to not increase the model order to avoid real-time implementation issues.

Fig. 4 depicts the tank water height validation results. The dotted line is the measurement of the cool water height in the tank, and the solid line is the output of the tank model. Clearly, the tank model successfully captures the dynamic of the cool water height in the tank.

3) Campus Load Model: The campus load model has two subcomponents: "the Solar and Internal Load Predictor" and the "Building Thermal Load Predictor". The Solar and Internal Load Predictor uses time, date, and cloud coverage as inputs, and calculates inside and outside solar loads and internal load. The outside solar load reflects the solar energy on the outer surface of the building, while the inside solar load is the solar radiation into the building (e.g., sunshine through the windows into rooms). The internal load includes the heat from people, lights, and equipment. More details can be found in [14].

The Building Thermal Load Predictor predicts the cooling load of buildings. We use a simple RC model whose main components includes walls and windows which are conventionally modeled by using thermal resistances and thermal capacitors [8]. The model inputs are ambient temperature (T_{amb}), cloud coverage (β_{cloud}), outside solar load ($\dot{Q}_{\mathrm{Solar,out}}$), inside solar load ($\dot{Q}_{\mathrm{Solar,in}}$), internal load ($Q_{\mathrm{internal}}$), the indoor temperature set-point (T_{sp}), and date (t). The model internal states are the temperatures of the thermal masses ($T_{\mathrm{in}}, T_{\mathrm{out}}$) and the model output is the cooling load ($\dot{Q}_{\mathrm{Load}}$). More information can be found in [14]. The campus load model described above has the form

$$\dot{T}_{\mathrm{state}} = g(T_{\mathrm{state}}, \Phi),\ \dot{Q}_{\mathrm{Load}} = \mathrm{LOAD}(T_{\mathrm{state}}, \Phi) \tag{5}$$

where $T_{\mathrm{state}} = [T_{\mathrm{in}}; T_{\mathrm{out}}]$, and $\Phi = [t; \beta_{\mathrm{cloud}}; T_{\mathrm{amb}}; T_{sp}]$.

Fig. 5 shows the identification result. The proposed campus load model captures the main load dynamics in May 2009. However, the peak values are not well modeled during the high load sessions and the campus load is slightly over predicted by the model for low load period of time. This can be improved by using a different set of parameters for different level of campus load.

The identified campus load model is validated by using load measurements from June 1–5, 2009. Fig. 6 presents the validation results. The measured campus load is depicted as the dotted line, and the solid line shows the campus load prediction by the

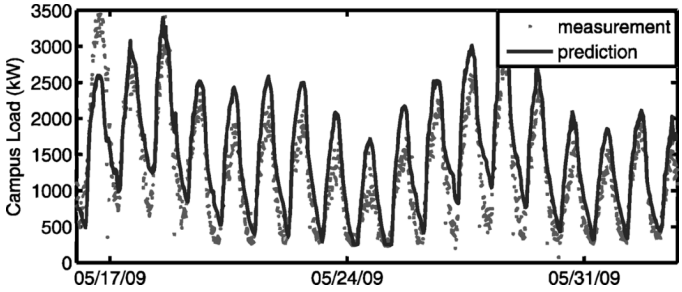

Fig. 5. Campus load model identification result (measured data in blue and simulation output in red).

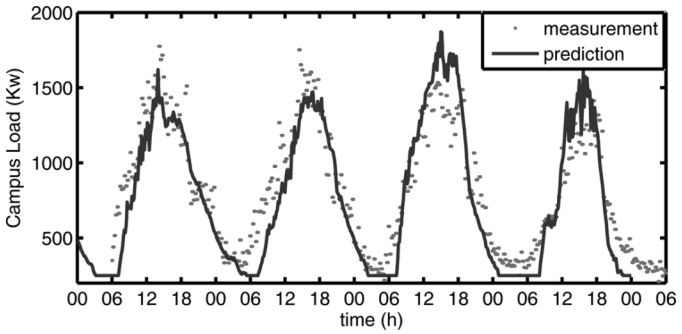

Fig. 6. Campus load model validation by using measurements from June 1–5, 2009.

proposed campus load model. The load dynamics are successfully captured by the proposed model.

4) Fan Coil Model: The fan coil models the heat exchange between the chilled water supplied to the campus and air in the buildings. Several fan coil models are available in the literature. A high fidelity simulation model has been developed in [20]. In this work we used the simplified semi-empirical model presented in [5] where the model inputs are the cooling load ($\dot{Q}_{\rm Load}$) calculated from campus load model described in Section II-B3, water supply temperature ($T_{{\rm cmp},s}$) and ambient temperature ($T_{\rm amb}$). The model outputs are water mass flow rate supplied to the campus ($\dot{m}_{{\rm cmp},s}$) and the return water temperature from the campus ($T_{{\rm cmp},r}$). The resulting semi-empirical model [5] can be compactly represented by using the following implicit function:

$$\text{FanCoil}(\dot{Q}_{\rm Load}, T_{{\rm cmp},s}, T_{\rm amb}, \dot{m}_{{\rm cmp},s}, T_{{\rm cmp},r}) = 0. \quad (6)$$

The fan coil model is implemented as a look up table to avoid solving implicit equations which are computational prohibitive for online optimization. We grid over the input space of the model $[\dot{Q}_{\rm Load}; T_{{\rm cmp},s}; T_{\rm amb}]$ and compute the corresponding outputs $[\dot{m}_{{\rm cmp},s}; T_{{\rm cmp},r}]$ by solving (6).

5) Weather Predictions: The weather predictions are downloaded from the National Digital Forecast Database via NOAA's National Weather Service. The weather data includes temperature and humidity for the following three days with a sampling time of two hours. The predicted weather information is used to predict the campus load.

C. Control Variables

1) $T_{\rm CWS,ref}(t)$: Reference temperature of water exiting cooling towers. The sampling rate is 1 hr.
2) $\dot{m}_{\rm CHWS,ref}(t)$: Mass flow rate of the chilled water supply. It is a disconnected set. The mass flow rate is 0 when chillers are off, and $[148, 235]$ kg/s while the chillers are operating. The sampling rate is 1 hr.
3) $T_{\rm CHWS,ref}(t)$: Reference temperature of water supplied by chillers. The sampling rate is 1 hr.
4) t_s (t_f): Start-up (Shut-down) time of chillers and cooling towers. The sampling rate is 1 day.

D. Measured Variables

There are five variables measured as follows.
1) $T_{\rm CHWR}$: Temperature of the water returning to the chillers.
2) $T_{\rm amb}$: Ambient temperature.
3) $T_{\rm CHWR}$: Temperature of the water flowing back to the chillers.
4) T_a (T_b): Temperature of the warm (cool) water in the tank.
5) z_a (z_b): Height of the warm (cool) water in the tank above (below) the thermocline.

E. Constraints

The following constraints avoid the malfunction of the system components.
1) $T_{\rm CWS,ref} \in [288, 295]$ K, $T_{\rm CHWS,ref} \in [276.5, 280.4]$ K, $T_{\rm CHWR} \in [283, 295]$ K, $z_b \in [0.3, 1] z_{\rm tank}$.
2) $\dot{m}_{\rm CHWS,ref}(t) \in \begin{cases} [148, 235] \text{ kg/s}, & \text{if } t_s \geq t \geq t_f \\ \{0\}, & \text{else.} \end{cases}$

The whole system has been designed to work properly only if such constraints are satisfied.

F. Model Summary

By collecting (2)–(6) and discretizing the system with sampling rate of one hour, the dynamic equations can be compacted as

$$x(t + \Delta t) = f(x(t), u(t), \Phi(t), t) \quad (7a)$$
$$y(t) = g(x(t), u(t - \Delta t), \Phi(t), t) \quad (7b)$$

where $u(t) = [T_{\rm CWS,ref}; \dot{m}_{\rm CHWS}; T_{\rm CHWS,ref}] \in \mathbb{U}$, $x(t) = [U_a; U_b; z_a; z_b; T_{\rm in}; T_{\rm out}]$, and $y(t) = [T_{\rm CHWR}; z_b] \in \mathbb{Y}$. $\mathbb{U}$ and $\mathbb{Y}$ are the sets of feasible control inputs and feasible outputs, respectively, defined in Section II-E.

III. MPC Problem Formulation

This section presents the design of a robust low-complexity MPC controller. The controller's objective is to find the optimal control sequence that satisfies the required cooling load, minimizes electricity bill and maximizes the coefficient of performance (COP). The electricity bill is defined as

$$\text{Bill}(t) = C(t)\text{Power}(x(t), u(t))\Delta t \quad (8)$$

where $\text{Power}(x, u)$ is the electrical power consumption as a function of states and inputs defined in Section II-B1; $C(t)$ is

the price of electricity (by the kilowatt/hour) at time t (details can be found in [14]).

The COP is calculated by

$$\mathrm{COP}(t) = \frac{\dot{m}_{\mathrm{CHWS}}(t) C_p (T_{\mathrm{CHWR}}(t) - T_{\mathrm{CHWS}}(t))}{\mathrm{Power}(x(t), u(t))}. \quad (9)$$

COP captures the efficiency of the central plant, i.e., the amount of thermal energy (J) generated by the central plant with one Joule of electrical energy.

Consider the following optimization problem:

$$J^\star(x(t), t) = \min_{\hat{u}_{0|t}, \ldots, \hat{u}_{M-1|t}, t_s, t_f} \sum_{k=1}^{N} \mathrm{Bill}(k\Delta t|t) \quad (10a)$$

$$\text{s.t. } y_{k\Delta t|t} \in \mathbb{Y}, \ \forall k = 1, 2, \ldots, N-1 \quad (10b)$$

$$u_{k\Delta t|t} \in \mathbb{U}, \ \forall k = 0, 1, \ldots, N-1 \quad (10c)$$

$$y_{N\Delta t|t} \in \mathbb{Y}_f(t) \quad (10d)$$

$$[u'_{0|t}, \ldots, u'_{(N-1)\Delta t|t}]' = B \otimes I_m [\hat{u}'_{0|t}, \ldots, \hat{u}'_{M-1|t}] \quad (10e)$$

$$x_{(k+1)\Delta t|t} = f(x_{k\Delta t|t}, u_{k\Delta t|t}, \Phi_{k\Delta t|t}, k\Delta t) \quad \forall k = 0, 1, \ldots, N-1 \quad (10f)$$

$$y_{k\Delta t|t} = g(x_{k\Delta t|t}, u_{(k-1)\Delta t|t}, \Phi_{k\Delta t|t}, k\Delta t) \quad \forall k = 1, 2, \ldots, N \quad (10g)$$

where $\otimes$ is the operation of Kronecker tensor product, $\mathbb{Y}_f(t)$ is a time-varying terminal constraint, $\Delta t = 1$ hr, $\mathrm{Bill}(t)$ is the function described in (8) to calculate the central plant energy bill, and M is the number of blocking moves along the control prediction horizon. In (10) $x_{k\Delta t|t}$ denotes the state vector at time $t + k\Delta t$ predicted at time t obtained by starting from the current state $x_{0|t} = x(t)$ and applying the input sequence $u_{0|t}, \ldots, u_{(N-1)\Delta t|t}$ to the system model (10f).

Let $U^\star_{0\to(N-1)\Delta t|t} = \{u^\star_{0|t}, \ldots, u^\star_{(N-1)\Delta t|t}\}$ be the optimal solution of problem (10) at time t, and $J^\star_t(x(t))$ the corresponding value function. Then, the first element of $U^\star_{0\to(N-1)\Delta t|t}$ is implemented to the system (7): $u(t) = u^\star_{0|t}$. The optimization problem (10) is repeated at $t + \Delta t$, with the updated state $x_{0|t+\Delta t} = x(t + \Delta t)$, yielding a *moving or receding horizon control* strategy. The proposed MPC controller uses a move blocking strategy (10e) to reduce the computational time required for its real time implementation. Details are discussed in the following section.

A. Move Blocking Strategy

The prediction horizon of the proposed MPC controller is 24 hr, and the control sampling time is 1 hr. As a result, there would be a total of 74 optimization variables as there are 3 control inputs with sampling time of 1 hr and two with sampling time of 1 day. It is common practice to apply a move blocking strategy to reduce the degrees of freedom [19]. The basic idea is to fix the input or its derivatives to be constant over several time steps.

In this brief, we are using a variant of the standard move blocking strategy called moving window blocking (MWB) and proposed in [4]. The main idea of the implemented MWB is to adopt a time-varying and periodic blocking strategy. At every time instance, only the lengths of the first and last blocks are modified in order to keep feasibility of shifted optimal sequences. By using this MWB strategy persistent feasibility is guaranteed for a periodic system and computational complexity is reduced. Details of the algorithm can be found in [4].

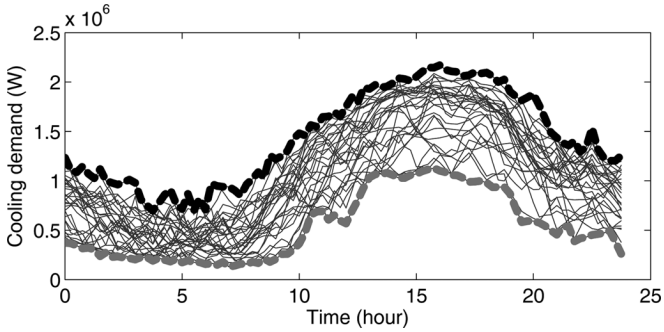

Fig. 7. Campus Load [W] from June–October, 2008.

B. Terminal Constraints

It is well known that stability and feasibility are not ensured by the MPC law without terminal cost and terminal constraints [16]. Usually the problem is augmented with a terminal cost and a terminal constraint set $\mathbb{Y}_f$. Typically $\mathbb{Y}_f$ is a robust control invariant set [16]. A robust control invariant set $\mathbb{P}$ enjoys the following property: if the system initial state belongs to the set $\mathbb{P}$, then the system can be controlled to be in $\mathbb{P}$ at all future time instants and for all admissible disturbances. It is well known that by using a robust control invariant terminal set $\mathbb{Y}_f$, the persistent feasibility of the MPC strategy is guaranteed (i.e., if Problem (10) is feasible for a given x_0, then it is feasible for all $t \geq 0$). Definitions and properties of invariant set can be found in [1], [16]. A treatment of sufficient conditions which guarantees persistent feasibility of MPC problems goes beyond the scope of this work and can be found in the survey [16].

We use historical data of $T_{\mathrm{cmp},s}$, $T_{\mathrm{cmp},r}$ and $\dot{m}_{\mathrm{cmp},s}$ in order to compute the possible range of $\dot{Q}_{\mathrm{Load}}$ calculated as

$$\dot{Q}_{\mathrm{Load}} = \dot{m}_{\mathrm{cmp},s} C_p (T_{\mathrm{cmp},r} - T_{\mathrm{cmp},s}) \quad (11)$$

Fig. 7 plots historical daily campus load during June–October, 2008. The goal was to obtain a good approximation of worst case load by looking at the months in the previous year with same weather behavior of the period during which experimental tests were conducted. Clearly the proposed methodology is independent of this choice. One can observe from Fig. 7 that it is reasonable to model the admissible campus load as a periodic disturbance with periodic envelope constraints (the bounds corresponds to the thicker lines in Fig. 7).

Since the disturbance is periodic, the idea proposed by the authors of [2] can be applied to the proposed MPC controller. The invariant set will be time variant and periodic with the same period as the disturbances. In order to guarantee that the tank has enough cold water to satisfy the demand, we use the algorithm proposed in [2] to calculate the controlled periodic invariant (CPI) set for the system described in (4a). The system for calculating the CPI set is a simple buffer (4a) subject to the constraints in Section II-E and the periodic disturbance modeled in Fig. 7.

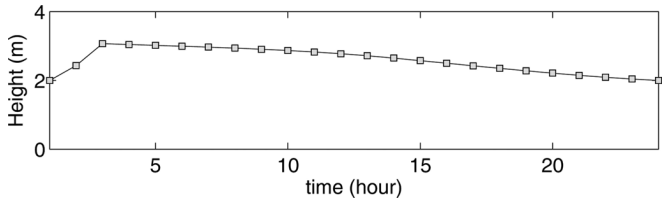

Fig. 8. Lower bound $b(t)$ of the CPI set $\mathbb{Y}_f(t)$ in (12).

We implemented the algorithm proposed in [2] and Fig. 8 plots the lower bound $b(t)$ of the computed periodic set $\mathbb{Y}_f(t)$

$$\mathbb{Y}_f(t) = \{z_b(t) : b(t) \leq z_b(t) \leq z_{\text{tank}}\}. \tag{12}$$

If the height $z_b(t)$ of the cooler water in the tank at time t is greater than the lower bounds $b(t)$, there exists a feasible feedback control law that will satisfy any disturbance belonging to the envelope in Fig. 7 without violating the constraints in Section II-E.

IV. Experimental Setup

The MPC controller outlined in Section III has been implemented at UC Merced. The detailed experimental setup is described below. The MPC controller computes the set points for cooling towers, chillers and the thermal storage tank at the central plant. Because of lower level control loops, the closed loop system indirectly affects all the components of the campus including the pumps and fan coils of the distribution system.

The MPC algorithm is implemented in MATLAB and running in real-time on a Pentium 4 Intel processor. The average computational time for solving an optimization problem was 20 min which ensured real-time implementation with the chosen 1-hr sampling time. The MPC algorithm receives and sends data to the campus through the building automation system "Automated Logics Web Control" (ALC) system.

V. Experiment

The following four scenarios have been studied in order to evaluate the performance of the MPC controller.

S1) Scenario 1 is the baseline performance. The plant is operated manually by using the policy defined by the plant managers. There is no optimal control algorithm involved. Rather, the control policy is based on the operators' experience. The data for experiment S1 are collected from May 27–31, 2009.

S2) Scenario 2 implements the MPC control (10) with the additional constraint that start time and stop time (t_s and t_f) can only be multiple of the sampling time (1 hr) [15]. The data for experiment S2 are collected from June 2–6, 2009.

S3) In Scenario 3 the plant is operated manually by using a modified policy defined by the plant managers. The modifications are extracted by observing the policy used by the MPC controller in S2. The data for experiment S3 are collected from June 8–12, 2009.

S4) Scenario 4 implements the MPC controller (10). The data for experiment S4 are collected from October 6–10, 2009.

TABLE I
Central Plant Performance Comparison (All Quantities Correspond to Daily Average)

	S1	S2	S3	S4
Energy Consumption [KJ]	$8.63e6$	$4.25e6$	$4.40e6$	$3.58e6$
Energy Generated [KJ]	$4.05e7$	$2.01e7$	$2.31e7$	$2.01e7$
COP	4.70	4.77	5.26	5.60
Bill [dollar]	$1.68e3$	$4.18e2$	$4.75e2$	$4.00e2$

In all four scenarios, the quantity of chilled water stored in the tank at the end of the experiment is forced to be equal to the one available at the beginning of the experiment. Despite the difference in time, the weather conditions during experiments S1 and S4 are similar. This allows us to fairly compare the MPC performance to the one obtained with the baseline control logic.

A. Comparison Metrics

Two metrics are defined to evaluate the performance of MPC: the electricity bills and the coefficient of performance (COP).

1) The daily electricity bill paid to operated the central plant, which is calculated as $\sum_{t=1}^{24} \text{Bill}(t)$, where $\text{Bill}(t)$ is defined in (8). By comparing the daily electricity bill we can quantify the cost savings generated by the MPC controller.
2) COP defined by (9). By comparing the COP between the four scenarios S1, S2, S3, and S4, we can better understand if MPC improves the efficiency of the central plant.

B. Discussion of Experimental Results

Next we compare the four experiments S1, S2, S3, and S4 by analyzing the performance of the central plant and the corresponding control profiles.

1) Performance Comparison: The performance of the central plant will be compared by using the metrics defined in Section V-A.

Table I lists the electrical energy consumption, thermal energy generated, COP and the electricity bill for experiments S1, S2, S3, and S4. We can observe that

- Comparing S1 with S2. The MPC controller has significantly reduced the daily electricity bill in experiment S2 by \$1265 compared to experiment S1. Meantime, the efficiency of central plant, COP, is also improved by 1.5%.
- Comparing S3 with S1. The electricity bill reduction is \$1205 and COP is increased by 11.9%.
- Comparing S4 with S3 and S1. The COP of the central plant reaches 5.60 in experiment S4, increased by 19.1% over baseline (S1). The daily electricity bill is reduced by \$75 when compared to S3 and by \$1280 when compared to S1.

The performance improvement is further discussed by looking at the implemented control profiles in the rest of the section.

2) Control Profile: Figs. 9–11 shows the control profiles for experiments S1, S2, S3, and S4, respectively. Table II lists the average values of the control set points during the charging time. Based on these information the following remarks can be drawn.

- The baseline control logics in S1 works as follow: condenser water supply temperature ($T_{\text{CWS,ref}}$) is set as low as possible so that the cooling towers always work at full load, chilled water supply temperature set point $T_{\text{CHWS,ref}}$ is fixed to 276.5 K, and the average mass flow rate $\dot{m}_{\text{CHWS,ref}}$

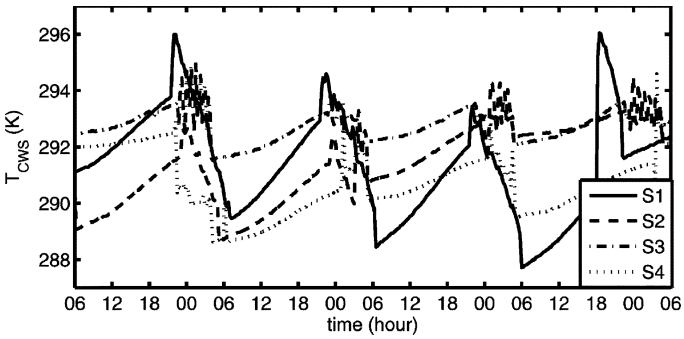

Fig. 9. Control input set points $T_{\mathrm{CWS,ref}}$.

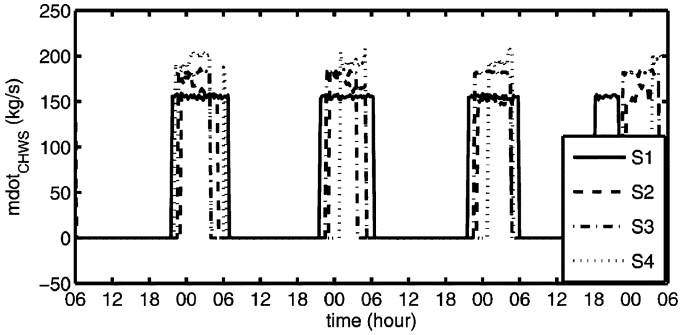

Fig. 10. Control input set points $\dot{m}_{\mathrm{CHWS,ref}}$.

is set to 150 kg/s. The operation schedule starts at 10 pm and ends when the tank is fully charged.

- The MPC controller in S2 applies higher condenser water supply temperature (T_{CWS}) for cooling towers than experiment S1. In the baseline control (experiment S1), the operators set the T_{CWS} as low as possible. This overloads the cooling towers, and a higher T_{CWS} can help balance the tradeoff between power consumed by the chilling system while meeting cooling loads.
- The MPC in S4, applies a desired condenser water supply temperature T_{CWS} of 293.1 K. However due to a lower level controller malfunctioning, T_{CWS} did not track its reference but was as low as 290.72 K in the first three days.
- During experiments S2 and S4, the central plant is working with shorter charging windows, and the average mass flow rate $\dot{m}_{\mathrm{CHWS}}$ is greater than the one used by the operators in S1.
- The set points of chilled water supply temperature $T_{\mathrm{CHWS,ref}}$ for S1, S2, S3, and S4 are reported in Fig. 11, and for S1, S2, and S3 scenarios, there is no noticeable difference.

We notice that experiment S3 improves COP over experiment S2 (with MPC in the loop). The reason is that the MPC in S2 assumes that start time and stop time [t_s and t_f in (10)] can only be multiple of the sampling time (one hour). Because of such coarse sampling time, a constant and high mass flow rate would overcharge the tank. As it can be observed in Fig. 10, the mass flow rate ($\dot{m}_{\mathrm{CHWS,ref}}$) in experiment S2 is high only at the beginning of the charging window. Then, it decreases in order to satisfy the load demand. Since for the specific scenario and chillers performance curves, a high COP is always obtained for higher mass flow rates ($\dot{m}_{\mathrm{CHWS,ref}}$), the decrease in $\dot{m}_{\mathrm{CHWS,ref}}$ erodes the efficiency of the central plant. This problem is fixed in

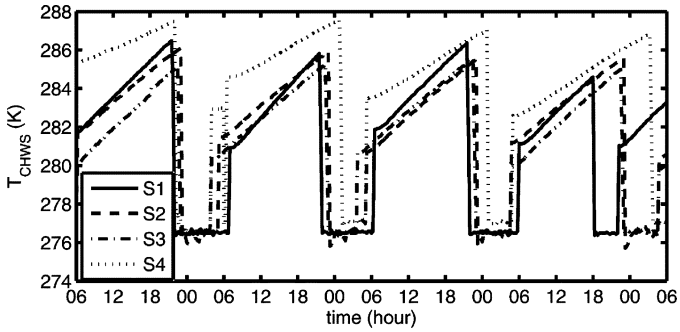

Fig. 11. Control input set points $T_{\mathrm{CHWS,ref}}$.

TABLE II
AVERAGE VALUES OF CENTRAL PLANT FLOWS AND TEMPERATURES DURING CHARGING TIME

	S1	S2	S3	S4
T_{CWS} [K]	289.0	292.3	293.2	290.72
$\dot{m}_{CHWS}$ [Kg/s]	152.6	158.2	178.0	187.0
T_{CHWS} [K]	276.7	276.4	276.9	278.6

experiment S4 where chillers start time and stop time (t_s and t_f) are allowed to assume any continuous value in the optimization problem (10). As a result, in scenario S4 a high flow $\dot{m}_{\mathrm{CHWS,ref}}$ is maintained over the charging period (see Fig. 10).

After experiment S2 the operators observed the behavior of the MPC and decided to apply maximum chilled water supply mass flow rate and set the condenser water supply temperature around 293.7 K. These two modification are used in scenario S3. As observed from Table II, the performance of the central plant, in terms of COP, is improved by 11.9% compared to their original baseline control S1.

C. Weather Dependence

The MPC performance is affected by the weather patterns. In order to better understand the potential improvement under a variety of weather conditions, an extensive simulation study over six months was performed. The proposed MPC in Section III was simulated in closed loop with the campus model in Section II. The campus load is estimated by using model presented in Section II-B3.

We performed extensive simulations from December 1, 2008 to July 1, 2009 by using the weather conditions at UC, Merced. Fig. 13 shows that the simulations cover a daily average ambient temperature from 278 K in winter to 300 K in summer. We note that under such a wide range of weather conditions, the COP with the MPC proposed in Section III constantly outperforms the COP of the baseline control (see Fig. 12). The missing points in Figs. 12–13 corresponds to missing data in the (corrupted) weather database.

Fig. 14 plots the correlation between the absolute COP improvement over baseline and the average ambient temperature during the charging time. The dashed line shows the upper bound of the COP improvement and the solid line is the lower bound. The MPC controller can achieve better COP improvement with average ambient temperature ranging from 285 to 291 K. This can be explained as follows. Low ambient temperatures limit the achievable condenser water temperature

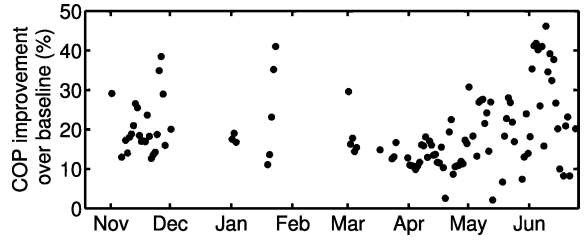

Fig. 12. COP improvement of MPC over baseline.

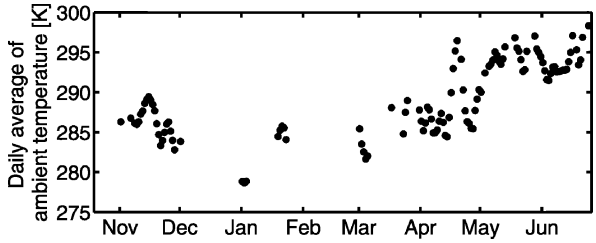

Fig. 13. Daily average of ambient temperature.

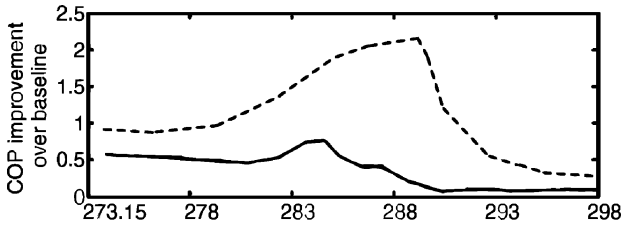

Fig. 14. Max (dashed line) and min (solid line) COP improvement as a function of average ambient temperature (K) during charging time.

(T_{CWS}) for cooling towers and, as pointed out in Section V-B2, higher condenser water temperature provides higher COP. On the other hand, higher ambient temperatures reduce the maximum COP achievable $\eta T_{\mathrm{CHWS}}/(T_{\mathrm{amb}} - T_{\mathrm{CHWS}})$, where η is the efficiency of the system, and $T_{\mathrm{CHWS}}/(T_{\mathrm{amb}} - T_{\mathrm{CHWS}})$ is the COP of an ideal Carnot compression refrigeration cycle [17].

VI. Conclusion

We presented the development of a model-based multi-variable controller for building cooling systems equipped with thermal energy storage by using prediction of weather conditions and buildings loads. We have been focusing on the architecture of the UC, Merced campus and shown that a simplified hybrid model can be used to predict the main behavior of the overall system. An MPC has been designed to optimize the scheduling and operation of the central plant to achieve lower electricity cost and better performance. Two main conclusions can be drawn from the experimental results. First, our study has enabled a 19.1% improvement of the plant COP compared to the original baseline logic. Second, the scheme has been used to confirm that some of the control profiles chosen by the operators and plant managers are very close to the control profiles suggested by MPC.

Acknowledgment

The authors would like to thank J. Elliott, S. Narayanan, and S. M. Oggianu for their constructive and fruitful discussions on the system modeling and control applications. They would also like to thank the anonymous reviewers for their helpful comments on the original version of the manuscript.

References

[1] F. Blanchini, "Set invariance in control—A survey," *Automatica*, vol. 35, no. 11, pp. 1747–1768, Nov. 1999.

[2] F. Blanchini and W. Ukovich, "Linear programming approach to the control of discrete-time periodic systems with uncertain inputs," *J. Opt. Theory Appl.*, vol. 78, no. 3, pp. 523–539, 1993.

[3] F. Borrelli, *Constrained Optimal Control of Linear and Hybrid Systems*. New York: Springer-Verlag, 2003, vol. 290.

[4] R. Cagienard, P. Grieder, E. C. Kerrigan, and M. Morari, "Move blocking strategies in receding horizon control," *J. Process Control*, vol. 17, no. 6, pp. 563–570, 2007.

[5] P. Haves, B. Hencey, F. Borrellli, J. Elliott, Y. Ma, B. Coffey, S. Bengea, and M. Wetter, "Model predictive control of HVAC systems: Implementation and testing at the University of California, Merced," Lawrence Berkeley National Laboratory (LBNL), Univ. California, Berkeley, 2010. [Online]. Available: https://gaia.lbl.gov/people/phaves/public/mpc%20doe%20cec%20report%20FINAL.docx

[6] E. Donaisky, C. H. C. Oliveira, R. Z. Freire, and N. Mendes, "PMV-Based predictive algorithms for controlling thermal comfort in building plants," in *Proc. IEEE Int. Conf. Control Appl. (CCA)*, 2007, pp. 182–187.

[7] C. Georgescu, A. Afshari, and G. Bornard, "Optimal adaptive predictive control and fault detection of residential building heating systems," in *Proc. 3rd IEEE Conf. Control Appl.*, 1994, pp. 1601–1606.

[8] M. Gwerder, B. Lehmann, J. Tödtli, V. Dorer, and F. Renggli, "Control of thermally-activated building systems (TABS)," *Appl. Energy*, vol. 85, no. 7, pp. 565–581, 2008.

[9] G. P. Henze, C. Felsmann, and G. Knabe, "Evaluation of optimal control for active and passive building thermal storage," *Int. J. Thermal Sci.*, vol. 43, no. 2, pp. 173–183, 2004.

[10] G. P. Henze, M. Krarti, and M. J. Brandemuehl, "Guidelines for improved performance of ice storage systems," *Energy Build.*, vol. 35, no. 2, pp. 111–127, 2003.

[11] G. P. Henze, J. Pfafferott, S. Herkel, and C. Felsmann, "Impact of adaptive comfort criteria and heat waves on optimal building thermal mass control," *Energy Build.*, vol. 39, no. 2, pp. 221–235, 2007.

[12] J. H. Lee, M. Morari, and C. E. Garcia, "State-space interpretation of model predictive control," *Automatica (J. IFAC)*, vol. 30, no. 4, pp. 707–717, 1994.

[13] Z. Liao and A. L. Dexter, "An inferential model-based predictive control scheme for optimizing the operation of boilers in building space-heating systems," *IEEE Trans. Control Syst. Technol.*, vol. 18, no. 5, pp. 1092–1102, Sep. 2010.

[14] Y. Ma, F. Borrelli, B. Hencey, B. Coffey, S. Bengea, P. Haves, A. Packard, and M. Wetter, "Model predictive control for the operation of building cooling systems," Univ. California, Berkeley, 2010. [Online]. Available: http://www.mpc.berkeley.edu/people/yudong-ma/files/UCMercedTCSTPapertexVersion8.pdf?attredirects=0

[15] Y. Ma, F. Borrelli, B. Hencey, A. Packard, and S. Bortoff, "Model predictive control of thermal energy storage in building cooling systems," in *Proc. 48th IEEE Conf. Dec. Control Held Jointly with the 28th Chinese Control Conf. (CDC/CCC)*, 2009, pp. 392–397.

[16] D. Q. Mayne, J. B. Rawlings, C. V. Rao, and P. O. M. Scokaert, "Constrained model predictive control: Stability and optimality," *Automatic*, vol. 36, no. 6, pp. 789–814, Jun. 2000.

[17] American Society of Heating, Refrigerating and Air-Conditioning Engineers, Inc., Atlanta, GA, "2009 Ashrae Handbook—Fundamentals (i-p Edition)," 2009.

[18] F. Oldewurtel, D. Gyalistras, M. Gwerder, C. N. Jones, A. Parisio, V. Stauch, B. Lehmann, and M. Morari, "Increasing energy efficiency in building climate control using weather forecasts and model predictive control," presented at the Clima—RHEVA World Congr., Antalya, Turkey, May 2010.

[19] S. J. Qin and T. A. Badgwell, "An overview of industrial model predictive control technology," *Control Eng. Pract.*, vol. 93, pp. 232–256, 1997.

[20] M. Wetter, "Simulation model: Finned water-to-air coil without condensation," LBNL, Berkeley, CA, Tech. Rep. 42355, 1999.